Grille flow-generated sound test data

Device ref	Grille description	Grille dimensions (rectangular duct), m	Grille strut type	Grille strut dimension* d, mm
A	Orthogonal metal mesh (25 mm square openings)	1.0 × 0.5	Round	2.5
B	Asymmetric metal mesh (non-uniform rhomboidal openings)	1.0 × 0.5	Round	2.5
C	Glass-reinforced plastic orthogonal 'eggcrate' grid (~50 mm square openings)	1.0 × 0.5	Flat (parallel to flow)	4.0
D	Machined slot-perforated metal plate (rectangular openings ~300 mm length, varying width)	1.1 × 1.1	Flat (perpendicular to flow)	5.0**
E	Orthogonal metal mesh (rectangular openings)	0.6 × 0.6	Round	3.0
*Estimated based on available information and adjusted according to model peak frequency fit. **Slot widths varied slightly, imposing a corresponding variation in the strut width. A single, representative, value had to be estimated for use in the prediction modelling.				

Table 1: Grille test details

Dev ref	Dir	T_C, °C	U, ms^{-1}	ΔP, Pa	63 Hz	125 Hz	250 Hz	500 Hz	1 kHz	2 kHz	4 kHz	8 kHz
A	1	22.6	10.0	29.0	56.3	54.1	51.7	55.7	58.6	54.3	43.7	35.4
A	1	22.6	25.0	191.0	79.1	75.7	74.7	76.4	77.4	80.6	74.9	67.6
A	1	22.6	40.0	517.0	85.7	84.7	85.1	87.1	87.4	89.3	89.6	82.9
A	1	22.6	55.0	1007.0*	100.7	94.4	92.0	93.7	95.0	96.8	98.4	95.4
A	2	23.6	10.0	31.0	58.3	55.7	52.0	54.7	58.2	54.0	44.3	35.6
A	2	23.6	25.2	226.0	74.5	76.0	74.2	75.9	76.8	82.9	75.2	69.4
A	2	23.6	40.2	604.0	85.7	85.8	85.3	87.2	88.1	91.3	93.9	85.7

Dev ref	Dir	T_C, °C	U, ms^{-1}	ΔP, Pa	63 Hz	125 Hz	250 Hz	500 Hz	1 kHz	2 kHz	4 kHz	8 kHz
A	2	23.6	55.0	1163.4*	100.7	94.5	92.5	94.2	95.0	96.8	100.6	97.2
B	1	22.7	10.0	25.0	56.2	53.7	52.6	53.7	54.3	48.7	41.8	33.3
B	1	22.7	25.0	180.0	78.0	75.0	73.2	75.2	76.4	80.8	72.0	66.7
B	1	22.7	40.2	454.0	96.0	87.1	85.4	87.3	87.3	88.2	95.6	81.8
B	1	22.7	55.0	885.3*	104.3	96.9	91.8	94.3	95.5	96.3	105.7	103.3
B	2	23.2	10.0	26.0	57.2	55.4	53.3	55.3	58.0	54.2	45.8	35.8
B	2	23.2	25.0	178.0	73.8	75.3	73.9	76.6	77.3	84.3	76.0	68.7
B	2	23.2	40.2	462.0	93.0	84.8	85.1	87.3	88.2	90.3	98.6	83.9
B	2	23.2	55.0	867.1*	100.7	94.4	92.0	94.9	95.4	97.1	107.0	105.1
C	1	22.7	10.0	69.0	64.1	66.7	69.3	69.6	65.6	62.7	52.1	46.0
C	1	22.7	25.0	442.0	80.8	81.5	87.7	93.7	92.9	91.8	81.6	74.6
C	1	22.7	40.2	1153.0	87.8	90.7	96.7	103.2	105.6	105.7	97.9	91.3
C	1	22.7	49.0	1718.0*	94.5	93.6	99.6	107.4	110.8	111.4	105.2	98.0
C	2	23.3	10.0	43.0	57.3	57.9	58.3	61.4	58.9	59.2	51.2	43.2
C	2	23.3	25.0	288.0	74.0	76.8	82.8	84.8	85.3	84.1	78.4	72.1
C	2	23.3	40.2	753.0	83.8	83.8	93.2	97.2	96.5	98.3	92.3	86.2
C	2	23.3	49.0	1046.1*	91.0	90.1	98.0	102.4	101.9	103.4	99.0	93.7
C	2	23.3	55.0	1325.8*	100.7	94.4	100.3	105.3	104.9	106.4	102.9	97.2
D	1	-	4.4	55.0	55.7	61.6	57.0	51.5	50.1	47.3	39.8	29.8
D	1	-	4.2	48.0	55.7	60.2	55.8	50.3	48.9	45.7	38.0	27.3
D	1	-	4.1	46.0	55.9	59.9	55.4	50.1	48.8	45.2	37.4	27.1
D	1	-	3.5	34.0	54.4	53.8	49.6	45.2	44.2	38.3	29.3	18.1
D	1	-	3.1	24.0	53.6	48.1	43.3	40.4	39.5	31.5	20.5	11.1
D	1	-	2.3	15.0	46.4	40.7	36.1	34.4	30.6	18.9	5.2	8.0

Dev ref	Dir	T_C, °C	U, ms^{-1}	ΔP, Pa	63 Hz	125 Hz	250 Hz	500 Hz	1 kHz	2 kHz	4 kHz	8 kHz
D	2	-	4.5	57.0	55.5	63.1	57.8	52.1	50.0	47.1	40.7	31.1
D	2	-	3.9	43.0	54.2	59.0	52.9	47.8	45.6	41.8	33.8	22.1
D	2	-	3.6	36.0	53.1	56.6	50.5	45.7	43.6	38.8	30.0	18.9
D	2	-	3.1	26.0	51.1	50.6	44.6	40.9	38.5	31.3	21.3	14.6
D	2	-	2.4	17.0	47.3	40.3	36.8	34.0	30.3	19.7	10.1	7.4
E	1	-	5.0	10.0	40.1	36.9	38.2	34.6	30.4	27.1	21.3	24.4
E	2	-	5.0	38.0	42.3	42.0	42.2	42.8	38.0	34.8	27.7	25.3

*Pressure drop estimated using additional data and regression modelling as per Table 3 (values displayed with rounded precision).

A temperature of 20°C has been assumed for tests without reported temperature values.

Table 2: Grille flow-generated sound power test data

As noted in **Table 2**, pressure drop values were unavailable for some of the tests at higher flow velocities. Therefore, these values were estimated by using the available flow and pressure test data to fit 2nd order polynomial multiple linear regression models and predict the pressure drop values for the higher velocity tests. The models incorporated additional data points for which only flow data (not sound data) were reported, as summarised in **Table 3**.

Dev ref	Dir	T_C, °C	U, ms^{-1}	ΔP, Pa	Regression model*	Model fit R^2 (coefficient of determination)*
A	1	22.6	32.8	340.0	$\Delta Pa = 0.3645U^2 - 1.9602U + 12.153$	1.0000
A	2	23.6	32.8	386.0	$\Delta Pa = 0.4229U^2 - 2.3381U + 12.701$	0.9998
B	1	22.7	32.8	229.0	$\Delta Pa = 0.3751U^2 - 5.3903U + 47.109$	0.9635
B	2	23.2	32.8	303.0	$\Delta Pa = 0.2900U^2 - 0.1656U - 1.0193$	0.9999
C	1	22.7	32.8	764.0	$\Delta Pa = 0.7270U^2 - 0.6121U + 2.4918$	1.0000
C	2	23.3	32.8	510.0	$\Delta Pa = 0.4555U^2 + 0.7496U - 10.837$	0.9998

*Coefficients shown rounded to displayed precision.

Table 3: Additional flow data and regression models used to estimate pressure drop values indicated in Table 2

Jet sound emission similarity spectra formulae

The formulae for the narrowband, linear frequency resolution power spectral representation of the jet sound emission similarity spectra derived by Tam et al (45) are provided below as functions of frequency relative to the spectral peak for the large-scale (f_{L}) or fine-scale (f_{F}) turbulence spectrum — it should be noted that there are typographical errors contained in the original publication (45), which have been amended in the formulae presented below.

Large-scale power spectrum $10\log_{10}[X(f/f_{\mathrm{L}})]$:

$$10\log_{10}X = \begin{cases} 5.64174 - 27.7472\log_{10}\left(\frac{f}{f_{\mathrm{L}}}\right); & \frac{f}{f_{\mathrm{L}}} \geq 2.5 \\ \left\{1.06617 - 45.299040\log_{10}\left(\frac{f}{f_{\mathrm{L}}}\right) + 21.40972\left[\log_{10}\left(\frac{f}{f_{\mathrm{L}}}\right)\right]^2\right\}\log_{10}\left(\frac{f}{f_{\mathrm{L}}}\right); & 2.5 > \frac{f}{f_{\mathrm{L}}} \geq 1.0 \\ -38.19338\left[\log_{10}\left(\frac{f}{f_{\mathrm{L}}}\right)\right]^2 - 16.91175\left[\log_{10}\left(\frac{f}{f_{\mathrm{L}}}\right)\right]^3; & 1.0 > \frac{f}{f_{\mathrm{L}}} \geq 0.5 \\ 2.53895 + 18.4\log_{10}\left(\frac{f}{f_{\mathrm{L}}}\right); & 0.5 > \frac{f}{f_{\mathrm{L}}} \end{cases}$$

Equation 1

Fine-scale power spectrum $10\log_{10}[Y(f/f_{\mathrm{F}})]$:

$$10\log_{10}Y = \begin{cases} 29.77786 - 38.16739\log_{10}\left(\frac{f}{f_{\mathrm{F}}}\right); & \frac{f}{f_{\mathrm{F}}} \geq 30 \\ -11.8 - \left\{27.2523 + 0.8091863\log_{10}\left(\frac{f}{10f_{\mathrm{F}}}\right) + 14.851964\left[\log_{10}\left(\frac{f}{10f_{\mathrm{F}}}\right)\right]^2\right\}\log_{10}\left(\frac{f}{10f_{\mathrm{F}}}\right); & 30 > \frac{f}{f_{\mathrm{F}}} \geq 10 \\ -\left[8.1476823 + 3.6523177\log_{10}\left(\frac{f}{f_{\mathrm{F}}}\right)\right]\left[\log_{10}\left(\frac{f}{f_{\mathrm{F}}}\right)\right]^2; & 10 > \frac{f}{f_{\mathrm{F}}} \geq 1.0 \\ \left[-1.0550362 + 4.9774046\log_{10}\left(\frac{f}{f_{\mathrm{F}}}\right)\right]\left[\log_{10}\left(\frac{f}{f_{\mathrm{F}}}\right)\right]^2; & 1.0 > \frac{f}{f_{\mathrm{F}}} \geq 0.15 \\ -3.5 + \left\{11.874876 + 2.1202444\log_{10}\left(\frac{20f}{3f_{\mathrm{F}}}\right) + 7.5211814\left[\log_{10}\left(\frac{20f}{3f_{\mathrm{F}}}\right)\right]^2\right\}\log_{10}\left(\frac{20f}{3f_{\mathrm{F}}}\right); & 0.15 > \frac{f}{f_{\mathrm{F}}} \geq 0.05 \\ 9.9 + 14.91126\log_{10}\left(\frac{f}{f_{\mathrm{F}}}\right); & 0.05 > \frac{f}{f_{\mathrm{F}}} \end{cases}$$

Equation 2

The outputs from these formulae are shown in **Figure 1**:

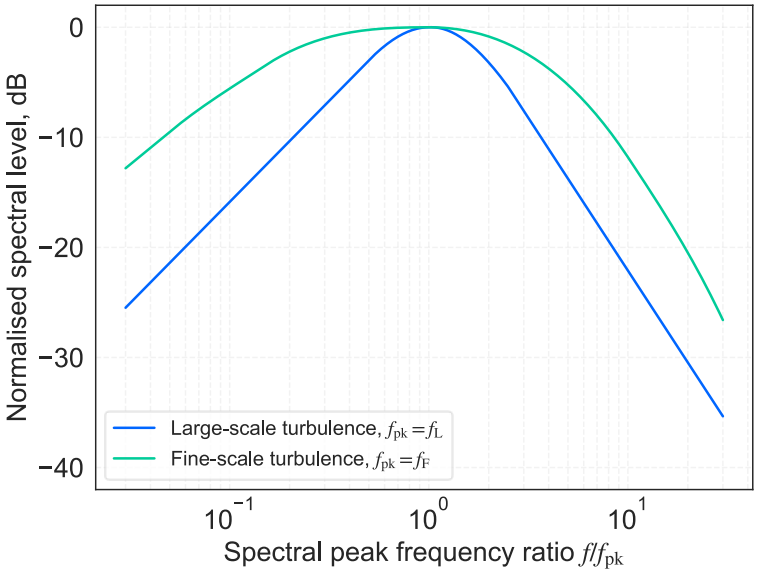

Figure 1: Narrowband jet sound emission similarity spectra developed by Tam et al (45) (linear frequency resolution, normalised to peak frequency level)